

1 **kinfitr: Reproducible PET Pharmacokinetic** 2 **Modelling in R**

3 **Granville J. Matheson¹**

4 ¹**Center for Psychiatry Research, Department of Clinical Neuroscience, Karolinska**
5 **Institutet & Stockholm Health Care Services, Stockholm County Council, Stockholm,**
6 **Sweden.**

7 Corresponding author:

8 Granville J. Matheson¹

9 Email address: `granville.matheson@ki.se`

10 **ABSTRACT**

11 Quantification of Positron Emission Tomography (PET) data is performed using pharmacokinetic models.
12 There exist many models for describing this data, each of which may describe the data better or worse
13 depending on the specific application, and there are both theoretical, practical and empirical reasons to
14 select any one model over another. As such, effective PET modelling requires a high degree of flexibility,
15 while effective communication of all steps taken through scientific publications is not always feasible.
16 Reproducible research practices address these concerns, in that researchers share analysis code, and
17 data if possible, such that all steps are recorded, allowing an independent researcher to reproduce the
18 results and assess their veracity. In this article, I present *kinfitr*: a software package for performing kinetic
19 modelling using the open-source R language, in a reproducible manner. The R community has a strong
20 culture of reproducible research, and the language consists of numerous tools which allow both effective
21 and easy sharing and communication of analysis code. The package is written in such a way as to allow
22 the analyst the freedom to use and rapidly exchange between approaches, and to assess goodness of
23 fit, with 14 different kinetic models currently implemented using a consistent syntax, as well as tools for
24 working with the data. By providing open-source tools for kinetic modelling, including documentation and
25 examples, it is hoped that this will extend access to methodology for research groups lacking software
26 engineering expertise, as well as simplify and thereby encourage transparent and reproducible reporting.

27 **INTRODUCTION**

28 Positron emission tomography (PET) is an *in vivo* neuroimaging method with high biochemical sensitivity
29 and specificity: it is an essential tool for the study of the neurochemical pathophysiology of mental
30 and neurological disease as well as for evaluating pharmacological treatments. This method allows for
31 accurate quantification of picomolar concentrations, thereby allowing insights which are not possible
32 using any other *in vivo* imaging modality. PET is, however, prohibitively expensive, often costing in
33 excess of USD 10 000 per measurement, and additionally involves exposure of participants to harmful
34 radioactivity. For this reason, accurate quantification is imperative in order to maximise the scientific
35 value of each measurement, as well as to minimise the number of participants who must be exposed to
36 radiation in order to answer the scientific question at hand.

37 Receptor PET quantification involves measuring the radioactivity in the tissue of interest following
38 the injection of a radiolabelled ligand into the blood. For fully quantitative PET imaging, radioactivity
39 concentrations are measured over time, giving rise to a time activity curve (TAC). By examining the
40 dynamics of radioactivity concentrations as the ligand enters and exits the tissue, the researcher is able to
41 fit a model with which she can obtain information about the pharmacokinetics and binding of the ligand,
42 and thereby assess the concentration of the relevant protein. The most common use of PET modelling
43 involves the quantification of a static quantity of interest, which is estimated using a model fitted to the
44 entire dynamic time-course of measurements in any given region. This is in contrast with fMRI, for which
45 each 3D image within the time series represents the quantity of interest. The model used to perform
46 PET quantification is therefore of tremendous importance for the later statistical comparison using the

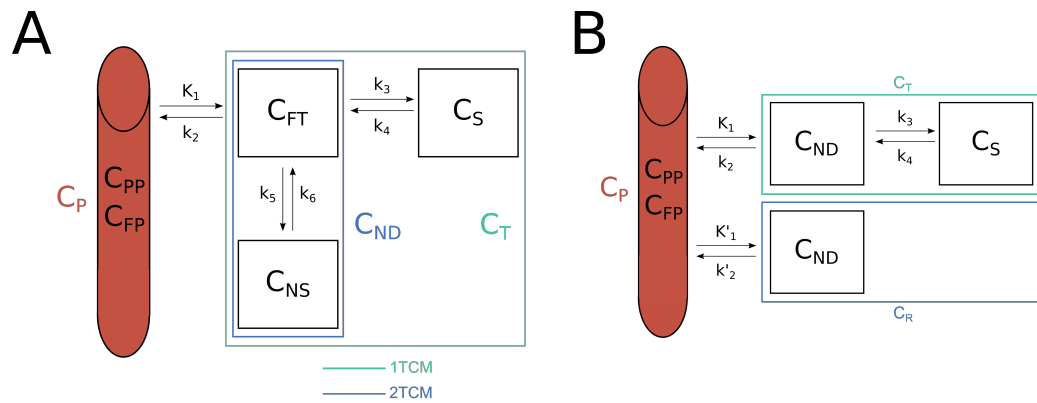


Figure 1. Compartmental models are the basis of PET kinetic modelling. For both panels, C represents the radioactivity concentrations within each compartment. The red cylinder on the left of each panel represents the arterial blood, containing plasma (P). Within the plasma, the radiotracer is either free (FP), or bound to plasma proteins (PP). The black boxes represent the compartments. TCM refers to Tissue Compartment Model. A. The three tissue compartment model is the basis for the two- and one-tissue compartment models: transfer between certain compartments are assumed to be sufficiently rapid that they can be considered as single compartments for the two- and one-tissue compartment models (coloured boxes). The compartments include FT free tracer, NS non-specifically bound, S specifically bound, T total, and ND non-displaceable. B. Reference region models consider the total concentration of radiotracer in the target T and in the reference region R, and assume that the non-displaceable concentration is equal in both regions, and that the specific binding in the reference region is equal to 0.

47 estimated quantity of interest.

48 There exist numerous different kinetic models for performing this quantification, which differ in a
 49 variety of important ways. Firstly, they differ in their specificity for the target binding, e.g. quantifying
 50 only the specific binding itself, as compared to quantifying the total binding, including non-specific
 51 binding (Innis et al. 2007). Secondly, they differ in their level of detail in their output, e.g. estimating
 52 only the estimate of the binding, compared to estimating all of the rate constants underlying that estimate.
 53 Thirdly, they differ in their relative degree of bias and variance, and hence their sensitivity to noise, i.e. how
 54 much they over- or under-fit the data). Fourthly, they differ in their assumptions about the behaviour of
 55 the radiotracer in the tissue, e.g. irreversible vs reversible binding, or the compartmental structure of the
 56 binding (Figure 1). These assumptions are usually only partially met in any given application, and care
 57 must be taken to ensure that the degree to which assumptions are not met does not bias the estimates
 58 in important ways (Salinas, Searle, and Gunn 2014). These differences are further complicated by the
 59 fact that the performance of different models may vary based on the properties of each specific tracer: a
 60 certain model may be more effective for certain cases than others, all else being equal.

61 For the modeller, there is no silver bullet. Rather, the model used to estimate the quantity of interest
 62 should be selected based on the radiotracer, as well as the research question and properties of the data
 63 set itself. This is further complicated by the myriad other analytical decisions which must be made prior
 64 to modelling, such as statistical weighting schemes, the application of partial volume effect correction,
 65 or the use of numerous ways that the blood data can be modelled too (the blood, blood-to-plasma ratio
 66 and parent fraction curves can all be modelled to derive improved estimates of the arterial input function
 67 curve, which can itself also be modelled). As such, effective PET modelling requires a high degree of
 68 flexibility, and the ability to rapidly exchange between different models. Effective communication of all
 69 steps taken through scientific publications, however, is not always feasible due to the large number of
 70 small decisions and results which are sometimes required to reach a decision about how best the data
 71 should be modelled. This complicates replication efforts and thereby retards scientific progress. This
 72 problem is by no means restricted to PET modelling, and is a property of the increasing complexity of
 73 computational analysis of scientific data more generally.

74 This general issue has led to calls among the broader scientific community for computational re-
 75 producibility, or more broadly *reproducible research* (RR), as a minimum standard for assessment of

76 scientific claims, i.e. that researchers share analysis code and, if possible, data. This ensures not only that
77 all steps are recorded, but this also allows an independent researcher to reproduce the results and assess
78 their veracity, as well as their sensitivity to various decisions taken during analysis. RR practices further
79 accelerate scientific progress, as novel methods can be readily validated, applied and extended by other
80 researchers using the shared code.

81 In this paper, I present *kinfitr*: a software package for performing PET kinetic modelling of TACs
82 using the R language. This tool both provides flexibility for effective modelling, while at the same time
83 being written in such a way as to promote transparency of this process. Further, by using the R language,
84 all code is open-source, and reproducible reporting is made easy by the extensive ecosystem of tools for
85 this purpose for the R language.

86 **DESCRIPTION**

87 The *kinfitr* package contains a host of tools for processing and modelling of PET TAC data, i.e. after the
88 raw image data has been transformed into vectors of radioactivity concentrations. The code is available at
89 <https://github.com/mathesong/kinfitr>.

90 **Model Functions**

91 There currently exist 14 models for TAC modelling (Gunn, Gunn, and Cunningham 2001; Rizzo et al.
92 2014; Logan et al. 1990, 1996; Ichise et al. 2002, 2003; Turkheimer et al. 2003; Patlak, Blasberg, and
93 Fenstermacher 1983; Patlak and Blasberg 1985; Todd Ogden, Zanderigo, and Parsey 2015; Lammertsma
94 and Hume 1996; Tomasi et al. 2008), including models which quantify binding relative to arterial plasma
95 input, reference regions, or semi-quantitative methods by which binding is quantified relative to the
96 injected dose of radioactivity and the mass of the participant. The models included and their descriptions
97 are included in Table 1. All models have associated plotting routines, which include representation of
98 weights, and the corresponding reference curve. Most models also produce standard errors of estimates,
99 estimated using the delta method when the parameters are not directly fitted.

Table 1. Kinetic models included in the package for modelling of time activity curves

Model	(Ir)reversible	Fit Method	t*	Input	Fit Parameters	Reference
One Tissue Compartment Model	Either	NLS		AIF	2-4	
Two Tissue Compartment Model	Either	NLS		AIF	4-6	
Two Tissue Compartment Model with Irreversible Trapping	Either	NLS		AIF	5-7	Rizzo et al., 2014
Logan Plot	Reversible	OLS	Required	AIF	1	Logan et al., (1990)
Ichise Multilinear Analysis 1	Reversible	OLS	Required	AIF	1	Ichise et al., (2002)
Ichise Multilinear Analysis 2	Reversible	OLS	Required	AIF	1	Ichise et al., (2002)
Multilinear Logan Plot	Reversible	OLS	Required	AIF	1	Turkheimer et al., (2003)
Patlak Plot	Irreversible	OLS	Required	AIF	1	Patlak et al., (1983)
Simultaneous Estimation of Non-Displaceable Binding	Reversible	NLS + GridSearch		AIF	1	Ogden et al., (2015)
Simplified Reference Tissue Model	Reversible	NLS		Reference Tissue	3	Lammertsma & Hume, (1996)
Simplified Reference Tissue Model with Blood Volumes	Reversible	NLS		Reference Tissue	4-5	Tomasi et al., (2008)
Non-Invasive Logan Plot	Reversible	OLS	Required	Reference Tissue	1	Logan et al., (1996)
Ichise's Multilinear Reference Tissue Model	Reversible	OLS	Optional	Reference Tissue	2	Ichise et al., (2003)
Ichise's Multilinear Reference Tissue Model 2	Reversible	OLS	Optional	Reference Tissue	1	Ichise et al., (2003)
Non-Invasive Multilinear Logan Plot	Reversible	OLS	Required	Reference Tissue	1	Turkheimer et al., (2003)
Patlak Reference Tissue Model	Irreversible	OLS	Required	Reference Tissue	1	Patlak et al., (1985)

100 **Model Fitting**

101 In addition to the standard implementations of all models (ordinary least squares for linear models, and
102 Levenberg-Marquardt algorithm for nonlinear models), all those which are fitted using nonlinear least
103 squares (NLS) have an additional option to be fit multiple times using different starting parameters: this is
104 useful when there are local minima within parameter space. Using the *nls.multstart* package (Padfield and
105 Matheson 2018), starting parameters can either be sampled either from a uniform distribution, or from a
106 grid, across parameter space to ensure that the best-fitting parameters are identified.

107 For most linear models, there is a t^* value which must be supplied. This value represents the point
108 at which linearity is reached. For all models for which a t^* value can be provided, there are included
109 functions for selecting which t^* value is most appropriate. As an intentional design decision, the selection
110 of the t^* is not automated: rather, the user is presented with R^2 values, percentage variance and changes
111 in binding estimates for each potential t^* value such that an appropriate value can be selected from
112 examining plots for several individuals to determine a t^* value for a sample.

113 **Blood preprocessing**

114 The *kinfitr* package contains a set of tools for preprocessing of blood data. Blood data can be read into
115 *kinfitr* directly and automatically from PET BIDS JSON files as *blooddata* objects. This contains the
116 raw data for the arterial blood, arterial plasma, blood-to-plasma ratio, parent fraction, and arterial input
117 function, as well as the models used to interpolate this data. These objects also contain the model which
118 will be used to interpolate this data. By default, the interpolation method is defined as piecewise linear
119 interpolation, but all curves can also be interpolated using nonlinear models. All of the data points,
120 interpolated curves and their combination to produce the final arterial input function can be visualised
121 using a *plot* command.

122 There are numerous nonlinear models available for the modelling blood curves, and a selection of
123 these models are included in the *kinfitr* package. For modelling of the parent fraction, the Hill, power,
124 exponential and cumulative inverse gamma functions models are included (Tonietto et al. 2016), as well
125 as the modification of the Hill function by Guo et al. (Guo et al. 2013). For modelling of blood or arterial
126 input function curves, the tri-exponential model (linear increase, followed by a tri-exponential decay),
127 as well as a spline model are available. Due to the large number, and *ad hoc* nature of many models for
128 modelling of blood curves, it is also possible to create new models which can be incorporated into the
129 *blooddata* object, or even to use the predictions from another external model (e.g. from another piece of
130 software).

131 Once the user is satisfied with the fits to the blood data, an *input* object can be created: this consists
132 of an interpolation of the curves into a common time series which can be used for kinetic modelling.
133 Additionally, if the user only has access to blood data which is already preprocessed, they can also bypass
134 the *blooddata* object, and directly interpolate the data into an *input* object.

135 **Included Data and Vignettes**

136 The *kinfitr* package contains two data sets in order to allow for the inclusion of examples with most
137 functions for demonstrating their uses. The first dataset, called *pbr28*, consists of TACs and blood data
138 from several individuals measured using $[^{11}\text{C}]\text{PBR28}$ from Matheson et al. (2017). This data includes 10
139 individuals, each measured twice in a test-retest study protocol, and includes TACs from six regions as
140 well as blood data. Blood data is provided both in processed form, as was used in Matheson et al. (2017),
141 but also in raw BIDS format. The second dataset, called *simref*, consists of a simulated dataset of 20
142 individuals which can be modelled using a reference region approach.

143 The package will also contain several vignettes which are currently under development, demonstrating
144 how the functions of the package can be used. This allows new users to quickly learn how to use the
145 package, and to allow them to get started by recycling, and reverse-engineering already-written code,
146 rather than beginning from scratch. The included vignettes will be as follows:

- 147 1. Reference Tissue Models
- 148 2. Arterial Input Models
- 149 3. Choosing a Suitable t^* in Linear Models
- 150 4. Pre-processing and Modelling of Blood Data

151 **Other Functions**

152 The package also contains a number of helper functions which can be used for the kinds of calculations
153 and processing steps which must often be performed to accompany TAC modelling. The package
154 includes a unit conversion function, for translating between any standard units of radioactivity to any
155 other, as well as for applying, and reversing, decay correction. For blood data collected using automated
156 blood sampling systems, the package offers dispersion correction. The package additionally methods for
157 estimating weights of TACs.

158 For models involving arterial input, the TAC data and arterial input data must be matched in time. All
159 of the “tissue compartment models” allow for additional fitting of the time delay between these curves, as
160 well as the blood volume fraction as additional parameters.

161 **Inputs and Syntax**

162 All tools within the *kinfitr* package have been designed to function with numeric vectors to as great an
163 extent as possible, as opposed to highly structured lists. This is an intentional design decision in order
164 to allow most functions within the package not to be reliant on having created specific data structures
165 in previous steps. Instead, users should be able to make use of functions from the package at whichever
166 stage of a given processing pipeline. Notable exceptions are those of *blooddata* and *input* objects, which
167 are created to make it easier to deal with blood data arising from a multitude of different sources, with
168 different time sequences.

169 Modelling functions have been written in such a way as to be as consistent with one another as
170 possible. Input arguments are the same between functions, and can be copied between the different
171 models. This allows users to quickly switch between different models with mostly, if not completely, the
172 same input arguments, thereby allowing a high degree of flexibility.

173 **Output**

174 Fit objects are created in order to be as extensive as possible. The specific model fits themselves are
175 included in the fit object, allowing them to be probed using methods such as AIC (Akaike Information
176 Criterion), BIC (Bayesian Information Criterion), *vcov* (return the variance-covariance matrix), afforded
177 by the stats package within the base R language. Additionally, *input*, weights and TAC data are included
178 after their time shifting to correspond with one another, as well as predicted values including which points
179 are to be considered before and after the t^* point for those models which contain a t^* . While this is
180 memory-intensive, this step allows users to rapidly identify the causes of a poor fit.

181 **The R Programming Language and Reproducibility**

182 One of the primary benefits of *kinfitr* is its being situated within the R programming language. R is an
183 open-source programming (R Core Team 2019) language designed by and for statisticians, and one of
184 the dominant languages used in Data Science. As such, it is excellent for performing data cleaning and
185 rearrangement before modelling, as well as for later statistical analysis and data visualisation. Further, it
186 makes it especially easy to implement additional methods which might be required to supplement the
187 tools available within *kinfitr* as a result of CRAN (the Comprehensive R Archive Network): the central
188 package repository for the R language, containing nearly 15 000 additional open-source packages.

189 Another key advantage of *kinfitr* being situated within the R programming language is access to the
190 extensive collection of tools for ensuring reproducibility. Rmarkdown (Xie 2017) allows for code, code
191 output (including plots) and text to be written side-by-side such that a new document can be generated
192 when the data changes. This is not limited to analysis reports: entire scientific articles (such as this one)
193 can be written within R (Allaire et al. 2019), where the plots and tables and even the values within the
194 text can be automatically updated when the document is re-compiled. While this may take more time
195 when first creating the report, the time savings in the long run can be dramatic, as all changes based on
196 alterations to processing or the underlying data are automatically incorporated. Furthermore, this is an
197 effective strategy to minimise errors when transferring figures between software, and, by being scripted,
198 allows for rapid identification and diagnosis of errors.

199 A final advantage is the fact that the R programming language and its packages are open-source.
200 This means that anyone can download it and use the same tools on their data. This also implies that
201 R and its packages can easily be run within virtual environments, either locally or in the cloud, with
202 ease. To this end, I have created a *kinfitr* Docker container, which allows users to download and run a
203 pre-installed version of R, Rstudio and *kinfitr* without needing to install or compile anything on their local

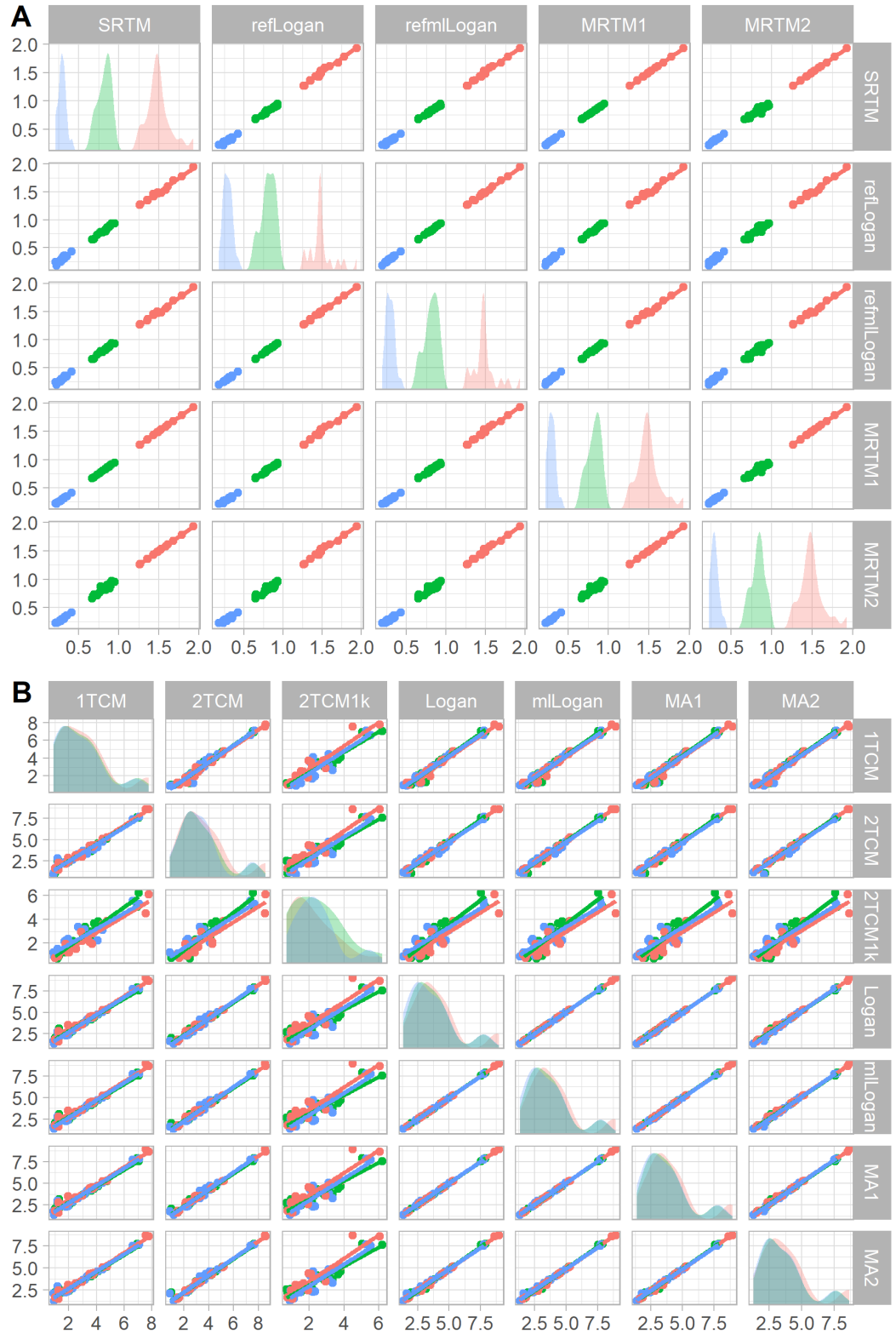


Figure 2. Comparison of primary outcomes between different models which can be applied to the sample data, with regions represented by colour, and regression lines fitted to each combination. A. Comparison of BP ND values obtained using the simref dataset. B. Comparison of VT values obtained using the pbr28 dataset.

204 machine other than Docker. It is available from the following link: https://hub.docker.com/r/matheson/kinfitr_docker.

206 Usage and validation

207 The *kinfitr* package has already been used in several scientific papers (Matheson et al. 2017, 2018;
208 Plavén-Sigraý et al. 2018; Chen, Goldsmith, and Ogden, n.d.; Stenkrona et al. 2019), and a full validation
209 is currently underway for the consistency of its outcomes compared to other software (Tjerkaski et al.,
210 *in prep*). In order to demonstrate basic usage of the *kinfitr* package, as well as to provide a preliminary
211 validation of its outcomes, the package was tested on the sample data included within the package. All
212 of the the relevant models for each dataset were applied for three regions and their estimated binding
213 outcomes are shown in Figure 2. From the figure, it is clear that the estimated parameters using each
214 model are highly correlated with one another. The full reproducible report is included in Supplementary
215 Code.

216 DISCUSSION

217 I have introduced the *kinfitr* package for analysis of PET TAC data using the R programming language.
218 This package contains tools for processing of PET data following image processing and extraction of time
219 activity curves, until the extraction of binding outcomes from the data and plotting of the model fits. By
220 being situated within the R programming language, this tool can benefit from the extensive collection
221 of other functions and packages within R, as well as the numerous tools for reproducibility, including
222 reproducible reporting and the use of pre-installed virtual computing environments.

223 The great expense and technical difficulty of PET, especially when blood data is also collected, as well
224 as the fact that participants are injected with harmful radioactivity, makes it imperative that the resulting
225 data is used in an optimal fashion. The *kinfitr* package makes it possible to make better use of PET data,
226 by providing researchers with access to a wide variety of kinetic models, and allows the results of this
227 modelling to be effectively, and transparently communicated in reproducible reports.

228 This package additionally makes it easier for multi-centre collaborative projects to harmonise their
229 data modelling procedures, as all analysis procedures and instructions are contained within the code
230 which can be shared between centres. By its use of BIDS PET structure for blood data, this means that
231 this complicated data originating from numerous different sources can be quickly and uniformly read and
232 analysed.

233 In summary, it is hoped that this package will help a researchers to perform PET modelling in a more
234 reproducible fashion, and to prioritise accuracy and transparency to a greater extent in their research.
235 Furthermore, by this project being open-source and hosted on GitHub, other users will also be able to add
236 additional tools and models to the software through pull requests, which can be merged to improve the
237 software package for everyone using it.

238 ACKNOWLEDGEMENTS

239 I gratefully thank the members of the PET group at Karolinska Institutet for their insightful comments and
240 feedback on *kinfitr* over the past years. Thank you especially to Pontus Plavén-Sigraý, Jonathan Tjerkaski,
241 Zsolt Cselényi (KI), Yakuan Chen (Columbia University) for their helpful suggestions, feedback, piloting
242 and bug reports. And thank you to Simon Cervenka for allowing me the freedom to work on developing
243 *kinfitr* during my studies.

244 REFERENCES

245 Allaire, J J, Yihui Xie, R Foundation, Hadley Wickham, Journal of Statistical Software, Ramnath
246 Vaidyanathan, Association for Computing Machinery, et al. 2019. *rticles: Article Formats for R*
247 *Markdown*. <https://github.com/rstudio/rticles>.

248 Chen, Y, J Goldsmith, and R Todd Ogden. n.d. “Nonlinear Mixed-Effects Models for PET Data.”
249 *IEEE Transactions on Biomedical Engineering*, 1. <https://doi.org/10.1109/TBME.2018.2861875>.

251 Gunn, R N, S R Gunn, and V J Cunningham. 2001. “Positron emission tomography compartmental
252 models.” *Journal of Cerebral Blood Flow and Metabolism* 21 (6): 635–52. <https://doi.org/10.1097/00004647-200106000-00002>.

- 254 Guo, Q., A. Colasanti, D. R. Owen, M. Onega, A. Kamalakaran, I. Bennacef, P. M. Matthews, E. A.
255 Rabiner, F. E. Turkheimer, and R. N. Gunn. 2013. "Quantification of the Specific Translocator Protein
256 Signal of 18F-PBR111 in Healthy Humans: A Genetic Polymorphism Effect on In Vivo Binding." *Journal*
257 *of Nuclear Medicine*. <https://doi.org/10.2967/jnumed.113.121020>.
- 258 Ichise, Masanori, Jieih-San Liow, Jian-Qiang Lu, Akihiro Takano, Kendra Model, Hiroshi Toyama,
259 Tetsuya Suhara, Kazutoshi Suzuki, Robert B Innis, and Richard E Carson. 2003. "Linearized reference
260 tissue parametric imaging methods: application to [11C]DASB positron emission tomography studies of
261 the serotonin transporter in human brain." *Journal of Cerebral Blood Flow and Metabolism : Official*
262 *Journal of the International Society of Cerebral Blood Flow and Metabolism* 23 (9): 1096–1112. <https://doi.org/10.1097/01.WCB.0000085441.37552.CA>.
- 264 Ichise, Masanori, Hiroshi Toyama, Robert B Innis, and Richard E Carson. 2002. "Strategies to
265 improve neuroreceptor parameter estimation by linear regression analysis." *J Cereb Blood Flow Metab* 22
266 (10): 1271–81. <https://doi.org/10.1097/00004647-200210000-00015>.
- 267 Innis, R B, V J Cunningham, J Delforge, M Fujita, A Gjedde, R N Gunn, J Holden, et al. 2007.
268 "Consensus nomenclature for in vivo imaging of reversibly binding radioligands." *J Cereb Blood Flow*
269 *Metab* 27 (9): 1533–9. <https://doi.org/10.1038/sj.jcbfm.9600493>.
- 270 Lammertsma, A A, and S P Hume. 1996. "Simplified reference tissue model for PET receptor studies."
271 *NeuroImage* 4 (3 Pt 1): 153–8. <https://doi.org/10.1006/nimg.1996.0066>.
- 272 Logan, Jean, Joanna S. Fowler, Nora D. Volkow, Gene-Jack Wang, Yu-Shin Ding, and David L.
273 Alexoff. 1996. "Distribution Volume Ratios without Blood Sampling from Graphical Analysis of PET
274 Data." *Journal of Cerebral Blood Flow & Metabolism* 16 (5): 834–40. <https://doi.org/10.1097/00004647-199609000-00008>.
- 276 Logan, Jean, Joanna S. Fowler, Nora D. Volkow, Alfred P. Wolf, Stephen L. Dewey, David J. Schlyer,
277 Robert R. MacGregor, et al. 1990. "Graphical analysis of reversible radioligand binding from time-activity
278 measurements applied to [N-11C-methyl]-(-)-cocaine PET studies in human subjects." *Journal of Cerebral*
279 *Blood Flow and Metabolism* 10 (5): 740–47. <https://doi.org/10.1038/jcbfm.1990.127>.
- 280 Matheson, Granville J, Pontus Plavén-Sigra, Anton Forsberg, Andrea Varrone, Lars Farde, and Simon
281 Cervenka. 2017. "Assessment of simplified ratio-based approaches for quantification of PET [11C]PBR28
282 data." *EJNMMI Research* 7 (1): 58. <https://doi.org/10.1186/s13550-017-0304-1>.
- 283 Matheson, Granville J, Pontus Plavén-Sigra, Anaïs Louzolo, Jacqueline Borg, Lars Farde, Predrag
284 Petrovic, and Simon Cervenka. 2018. "Dopamine D1 receptor availability is not associated with delusional
285 ideation measures of psychosis proneness." *bioRxiv*. <https://doi.org/10.1101/321646>.
- 286 Padfield, Daniel, and Granville J Matheson. 2018. "nls.multstart: Robust Non-Linear Regression
287 using AIC Scores." <https://cran.r-project.org/package=nls.multstart>.
- 288 Patlak, Clifford S, and Ronald G Blasberg. 1985. "Graphical evaluation of blood to brain barrier
289 transfer constants from multiple time uptake data. Generalizations." *Journal of Cerebral Blood Flow and*
290 *Metabolism* 5 (4): 584–90. <https://doi.org/10.1038/jcbfm.1985.87>.
- 291 Patlak, C. S., R. G. Blasberg, and J. D. Fenstermacher. 1983. "Graphical evaluation of blood-to-brain
292 transfer constants from multiple-time uptake data." *Journal of Cerebral Blood Flow and Metabolism* 3
293 (1): 1–7. <https://doi.org/10.1038/jcbfm.1983.1>.
- 294 Plavén-Sigra, Pontus, Granville J Matheson, Zsolt Cselényi, Aurelija Jučaitė, Lars Farde, and
295 Simon Cervenka. 2018. "Test-retest reliability and convergent validity of (R)-[11C]PK11195 outcome
296 measures without arterial input function." *EJNMMI Research*, 102. <https://doi.org/https://doi.org/10.1101/298992>.
- 298 R Core Team. 2019. "R: A Language and Environment for Statistical Computing." Vienna, Austria:
299 R Foundation for Statistical Computing. <https://www.r-project.org/>.
- 300 Rizzo, Gaia, Mattia Veronese, Matteo Tonietto, Paolo Zanotti-Fregonara, Federico E Turkheimer, and
301 Alessandra Bertoldo. 2014. "Kinetic Modeling without Accounting for the Vascular Component Impairs
302 the Quantification of [¹¹ C]PBR28 Brain PET Data." *Journal of Cerebral Blood Flow &*
303 *Metabolism* 34 (6): 1060–9. <https://doi.org/10.1038/jcbfm.2014.55>.
- 304 Salinas, Cristian a, Graham E Searle, and Roger N Gunn. 2014. "The simplified reference tissue model:
305 model assumption violations and their impact on binding potential." *Journal of Cerebral Blood Flow and*
306 *Metabolism : Official Journal of the International Society of Cerebral Blood Flow and Metabolism* 35 (2):
307 1–8. <https://doi.org/10.1038/jcbfm.2014.202>.
- 308 Stenkrona, Per, Granville J Matheson, Christer Halldin, Simon Cervenka, and Lars Farde. 2019.

- 309 “D1-Dopamine Receptor Availability in First-Episode Neuroleptic Naive Psychosis Patients.” *International Journal of Neuropsychopharmacology* 22 (7): 415–25. [https://doi.org/10.1093/ijnp/](https://doi.org/10.1093/ijnp/pyz017)
310 [pyz017](https://doi.org/10.1093/ijnp/pyz017).
- 312 Todd Ogden, R., Francesca Zanderigo, and Ramin V. Parsey. 2015. “Estimation of in vivo nonspecific
313 binding in positron emission tomography studies without requiring a reference region.” *NeuroImage* 108:
314 234–42. <https://doi.org/10.1016/j.neuroimage.2014.12.038>.
- 315 Tomasi, G., P. Edison, A. Bertoldo, F. Roncaroli, P. Singh, A. Gerhard, C. Cobelli, D. J. Brooks,
316 and Federico E Turkheimer. 2008. “Novel Reference Region Model Reveals Increased Microglial and
317 Reduced Vascular Binding of 11C-(R)-PK11195 in Patients with Alzheimer’s Disease.” *Journal of*
318 *Nuclear Medicine* 49 (8): 1249–56. <https://doi.org/10.2967/jnumed.108.050583>.
- 319 Tonietto, M, G Rizzo, M Veronese, M Fujita, S S Zoghbi, P Zanotti-Fregonara, and A Bertoldo.
320 2016. “Plasma radiometabolite correction in dynamic PET studies: Insights on the available mod-
321 eling approaches.” *J Cereb Blood Flow Metab* 36 (2): 326–39. [https://doi.org/10.1177/](https://doi.org/10.1177/0271678x15610585)
322 [0271678x15610585](https://doi.org/10.1177/0271678x15610585).
- 323 Turkheimer, Federico E., John A.D. Aston, Richard B. Banati, Cyril Riddell, and Vincent J. Cunn-
324 ham. 2003. “A linear wavelet filter for parametric imaging with dynamic PET.” *IEEE Transactions on*
325 *Medical Imaging* 22 (3): 289–301. <https://doi.org/10.1109/TMI.2003.809597>.
- 326 Xie, Yihui. 2017. *Dynamic Documents with R and knitr*. Chapman; Hall/CRC.